The American Journal of Pathology, Vol. 182, No. 6, June 2013

ELSEVIER

The American Journal of PATHOLOGY

ajp.amjpathol.org

BIOMARKERS, GENOMICS, PROTEOMICS, AND GENE REGULATION

Genome-Wide Methylation Analysis of Prostate Tissues Reveals Global Methylation Patterns of Prostate Cancer

Jian-Hua Luo,* Ying Ding,† Rui Chen,† George Michalopoulos,* Joel Nelson,‡ George Tseng,† and Yan P. Yu*

From the Departments of Pathology, Biostatistics,† and Urology,‡ University of Pittsburgh School of Medicine, Pittsburgh, Pennsylvania*

Accepted for publication February 1, 2013.

Address correspondence to Yan P. Yu, M.D., Ph.D., BST S-412, 200 Lothrop St., University of Pittsburgh School of Medicine, Pittsburgh, PA 15261. E-mail: ypyu@pitt.edu.

Altered genome methylation is a hallmark of human malignancies. In this study, high-throughput analyses of concordant gene methylation and expression events were performed for 91 human prostate specimens, including prostate tumor (T), matched normal adjacent to tumor (AT), and organ donor (OD). Methylated DNA in genomic DNA was immunoprecipitated with anti-methylcytidine antibodies and detected by Affymetrix human whole genome SNP 6.0 chips. Among the methylated CpG islands, 11,481 islands were found located in the promoter and exon 1 regions of 9295 genes. Genes (7641) were methylated frequently across OD, AT, and T samples, whereas 239 genes were differentially methylated in only T and 785 genes in both AT and T but not OD. Genes with promoter methylation and concordantly suppressed expression were identified. Pathway analysis suggested that many of the methylated genes in T and AT are involved in cell growth and mitogenesis. Classification analysis of the differentially methylated genes in T or OD produced a specificity of 89.4% and a sensitivity of 85.7%. The T and AT groups, however, were only slightly separated by the prediction analysis, indicating a strong field effect. A gene methylation prediction model was shown to predict prostate cancer relapse with sensitivity of 80.0% and specificity of 85.0%. These results suggest methylation patterns useful in predicting clinical outcomes of prostate cancer. *(Am J Pathol 2013, 182: 2028–2036; http://dx.doi.org/10.1016/j.ajpath.2013.02.040)*

Prostate cancer is one of the most prevalent malignancies among American men, with approximately 280,000 new cases diagnosed annually. Each year up to 28,050 patients with prostate cancer die in the United States alone, and mortality from prostate cancer is only second to lung carcinoma in the United States.[1] Although most prostate cancers are indolent and responsive to the available hormone therapies, a significant number of cases become hormone refractory and metastatic. The precise cause of prostate cancer progression has remained elusive, despite extensive research efforts and recent advances in our understanding of this disease. Comprehensive gene expression and genome analyses have suggested that a global pattern of gene expression and copy number alterations exist for prostate cancer.[2–4] The related gene products include critical molecules in signaling pathways, DNA replication, cell growth, cell cycle checkpoints, and apoptosis.[5–8]

Hypermethylation of the gene promoter is a well-known epigenetic event that silences gene expression and is a critical regulatory component in normal physiology, mediating gene imprinting for inactivation of the X chromosome[9] and tissue-specific gene expression,[10] and in pathological processes, mediating inactivation of tumor suppressor genes and promoting tumorigenesis.[11,12] Addition of a methyl group to the cytosine residue of CpG dinucleotides by methyltransferase creates a binding motif for methyl-cytosine binding proteins, methyl-CpG-binding domain (MBD) or methyl-CpG-binding protein 2 (MeCP2), which in turn produces steric hindrance at the CpG clusters located in the promoter regions to transcriptional activators or repressors.[13,14] Silencing of genes involved in cell cycle control, cell survival, DNA damage repair, and signal transduction is the characteristics of cancer cells.[15–23] There is a lack of global

Supported by the National Cancer Institute (grant RO1 CA098249 to J.-H.L.), the American Cancer Society (grant RSG-08-137-01-CNE to Y.P.Y.), and the University of Pittsburgh Cancer Institute.

J.-H.L., G.T., and Y.P.Y contributed equally to this work.

http://dx.doi.org/10.1016/j.ajpath.2013.02.040

correlation of CpG island methylation and gene expression in prostate cancer. To map the epigenetic regulation leading to altered expression of hundreds of genes in prostate cancer, we performed a genome-wide concordance analysis of gene methylation and expression in matched prostate tumor (T), benign prostate tissues adjacent to cancer (AT), and organ donor prostate without history of urological disease or any malignancy (OD). We found unique methylation profiles that distinguished the T, AT, and OD samples.

Materials and Methods

Genomic DNA Preparation

Ninety-one specimens of prostate cancer and adjacent benign prostate tissues and organ donor prostates were obtained from University of Pittsburgh Tissue Bank in compliance with institutional regulatory guidelines (Supplemental Table S1). To ensure high purity ($\geq$80%) of tumor cells, needle-microdissection was performed by pathologists to isolate the tumor cells from adjacent normal tissues ($\geq$3-mm distance from the tumor). For AT and OD samples, similar needle-microdissections were performed to achieve 80% epithelial purity. Genomic DNA of these T and AT tissues was extracted with a commercially available tissue and blood DNA extraction kit (Qiagen, Hilden, Germany). The protocols of tissue procurement and procedure were approved by Institution Board of Review of the University of Pittsburgh.

Immunoprecipitation and Amplification of Methylated DNA

Each DNA sample was divided into two aliquots of 250 ng and was digested with either StyI or Nsp1 (New England BioLabs, Ipswich, MA) at 37°C for 2 hours, followed by ligation to the corresponding StyI or Nsp1 adapters (Affymetrix, Santa Clara, CA) at 16°C for 16 hours. The two adapter-ligated DNAs were pooled and purified with an Amicon Ultra-centrifugation filter (Millipore, Billerica, MA). Fifty nanograms of the purified DNA in 450 μL of Tris-EDTA buffer were denatured by boiling in water for 10 minutes. Methylated DNA was then immunoprecipitated with 5 μg of anti−5-methylcytosine antibody (Zymo Research, Irvine, CA) in immunoprecipitation buffer (10 mmol/L $NaPO_4$, 140 mmol/L NaCl, and 0.05% Triton X-100, pH 7) by rocking at 4°C for 2 hours. The immunocomplexes were captured with magnetic bead-protein A/G (Millipore) by shaking at room temperature for 30 minutes. Three washes were performed with 1 mL of immunoprecipitation buffer, and additional washes with 300 μL of elution buffer heated to 50°C for 10 minutes were performed until the DNA in flow-through reached zero. Methylated DNA was then eluted from the beads with 100 μL of elution buffer heated to 75°C for 5 minutes. The eluted DNA was PCR amplified with titanium DNA polymerase and primer 002 from Affymetrix SNP 6.0 reagent kit, using 30 thermal cycles of 94°C for 30 seconds, 60°C for 45 seconds, and 65°C for 60 seconds. Amplification efficiency was assessed by resolving amplicons with 1% agarose gel electrophoresis. Samples were then purified and fragmented by incubating with DNase1 at 37°C for 35 minutes. The fragmented DNA samples (range, 100−200 bp) were biotin labeled with terminal transferase at 37°C for 4 hours and hybridized to Affymetrix human whole genome SNP 6.0 chips at 50°C for 19 hours. After washes with 6× SSPE (saline, sodium phosphate, EDTA) buffer and staining with phycoerythrin streptoavidin in an automated Affymetrix fluid station, the chips were scanned by Affymetrix GeneChip scanner 3000 7G.

Sample Baseline Genome Copy Number Analysis

To determine the baseline copy number of each sample, genome DNA of each sample was analyzed with the Affymetrix SNP 6.0 chip. Briefly, the adaptor ligated DNA was prepared from StyI and Nsp1 digestion as described in Immunoprecipitation and Amplification of Methylated DNA. The efficiency of amplification was verified by resolving amplicons with 1% agarose gel electrophoresis. The total amount of purified amplicons was in the range of 200 to 250 μg.[3,24] As described in the section above, the amplicons were DNAse1 fragmented, biotin labeled, hybridized to the Affymetrix SNP 6.0 chips, and processed for genome copy number analysis.

DNA Methylation Analysis

The hybridization signals of methylation-enriched DNA from 91 prostate tissues were analyzed by Partek Genomics Suite 6.6 (Partek, Inc., St. Louis, MO). Pair-wise copy number analyses of methylation-enriched DNA were performed with genome copy numbers of the unenriched DNA samples as baselines with criteria of marker numbers >10 and segment length >2000 bp. The segments that were detected as amplified or unchanged in comparison with the baseline copy number of the duplicate samples were considered to be enriched by the methylation-specific antibodies. These methylated fragments were then screened for CpG islands. Criteria of 50% C and G and expected CpG of 0.65 in a region of >200 bp was used to define a CpG island.[25−27] The CpG islands located in the region of 1000 bp upstream and 500 bp downstream of mRNA start site of a gene were designated as gene-associated CpG islands and were annotated through the UCSC (University of California Santa Cruz) genome build hg18. Microarray data location of Raw *.cel files of data will be available at Gene Expression Omnibus (*http://www.ncbi.nlm.nih.gov/geo*; accession number GSE45000).

Functional Analysis of Differentially Methylated Genes

The differential profiles of methylated genes were determined by comparing the CpG islands of T/OD, AT/OD, and T/AT, respectively. For each given gene-associated CpG island, the fraction of samples that were methylated was

tabulated for each group. A two-by-two contingency table was constructed and Fisher exact test was performed to detect the differential methylation of CpG islands. To examine whether the differential methylations of these gene-associated CpG islands were functional, the previously published U95 Affymetrix chip gene expression data of 130 cases of prostate cancer and donors (overlapping 75 of 91 samples of our present methylation analyses or 82%) were assessed.[4] The expression of each methylated gene was measured by calculating Pearson correlation coefficient between gene expression values[4,7] and methylation state vector (0,1) for each matched sample (33). The differential gene expression analysis that used a one-sided *t*-test was performed. A functional methylated gene was defined as a gene that was detected as hypermethylated in the analysis and was shown to have down-regulated gene expression. The difference in methylation status of these functional methylated genes between the compared groups was named as differential functional methylation events in the analysis. Significant differences in methylation and expression were indicated by a P value <0.05. Six sets of concordant genes were identified, including the hypermethylated and hypomethylated gene sets in T/D, AT/D, and T/AT groups.

Pathway Enrichment Analyses

Pathway analysis was performed for the six sets of concordant genes. A total of 2287 pathways were curated from MSigDB,[28] which contains information from Biocarta, Kyoto Encyclopedia of Genes and Genomes, Reactome, and Gene Ontology databases. The one-sided Fisher exact test (overrepresentation) was applied to calculate the statistical significance of pathway enrichment, and P values were corrected by the Benjamini-Hochberg procedure for multiple comparisons to calculate q values.

Statistical Prediction Model

Prediction (classification) analyses were performed for the four comparison groups: i) T versus OD, ii) AT versus OD, iii) T relapse versus T nonrelapse, and iv) T fast relapse versus slow relapse or nonrelapse. The conventional leave-one-out cross validation (LOOCV) approach was used to assess accuracy.[29] In LOOCV, one sample was left out for evaluation, and the remaining samples were used to construct a prediction model, which was then applied to the left-out sample evaluation for accuracy of prediction. The process was repeated until all of the samples were left out as test samples and the sensitivity and the specificity of the model for prediction of cancer or normal were achieved. The differentially methylated CpG islands were then applied as predictive features in the prediction model, and the top (parameter r) differentially methylated CpG islands (having equal number of differentially hypermethylation and hypomethylation) were selected for their significance in group comparisons of hypermethylation and hypomethylation with the use of Fisher exact test. To predict the left-out test sample, the percentage of concordance (parameter t) was calculated as a threshold for the methylation pattern in the training set with the prediction model in the top (r) differentially hypermethylated and hypomethylated CpG islands. Parameter (t) was used to balance the sensitivity and specificity trade-off in the prediction model. By varying p, a receiver operating characteristic (ROC) curve for classification was produced. In this analysis, the (r) that produced the best area under the curve (AUC) was selected, and the threshold p was determined by maximizing the Youden index (sensitivity + specificity − 1) for the best sensitivity and specificity trade-off and overall accuracy rate. The criterion used gave equal significance in sensitivity and specificity. To evaluate whether the prediction result was better than that obtained by a random approach, AUC was used as a test. Permutation analyses were performed to assess the statistical significance by random shuffling of the class labels (case and control) with new AUC values being calculated; this procedure was repeated 100 times to generate the null distribution. The P value was calculated as the percentage of 100 null AUCs from permutation and was greater than the observed AUC.

Methylation-Specific PCR

The genomic DNA from the same group of prostate tissue samples was treated with sodium bisulfite (Epitec bisulfite kit; Qiagen) at 95°C for 5 minutes, followed by 60°C for 4 hours, and desulfonated as described in the manufacturer's manual. The bisulfite-converted DNA was amplified as previously described,[30,31] using CDKN1c methylation-specific primers (5′-CGCGGTCGTTAATTAGTCGC-3′/5′-ACACAACGCACTTAACCTATAA-3′) or CDKN1c unmethylation-specific primers (5′-TTTGTTTTGTGGTTGTTAATTAGTTGT-3′/5′-ACACAACACACTTAACCTATAA-3′) with the following thermal cycling conditions: 40 cycles of 95°C for 30 seconds and 61°C for 1 minute, followed by 72°C for 2 minutes for methylation primers; or 40 cycles of 95°C for 30 seconds and 60°C for 1 minute, followed by 72°C for 2 minutes for unmethylation primers.

Results

To investigate the global DNA methylation patterns of prostate cancer, methylated DNA segments from the prostate genome were analyzed by detecting methylation-enriched DNA with Affymetrix human whole genome SNP 6.0. The methylated genome DNA samples were immunoprecipitated by antibodies specific for 5-methylcytidine, amplified, and hybridized to the SNP 6.0 chip. The methylation genome DNA profile of each sample was then analyzed with the whole genome DNA profile from the same sample as baseline. Regions of DNA were deemed methylated if they were detected as amplified or unchanged in comparison with the matched whole genome profile. A total of 34,413 genome segments were identified as methylated regions. To study whether all these genome segments were relevant to the regulation of gene expression, we screened each for the

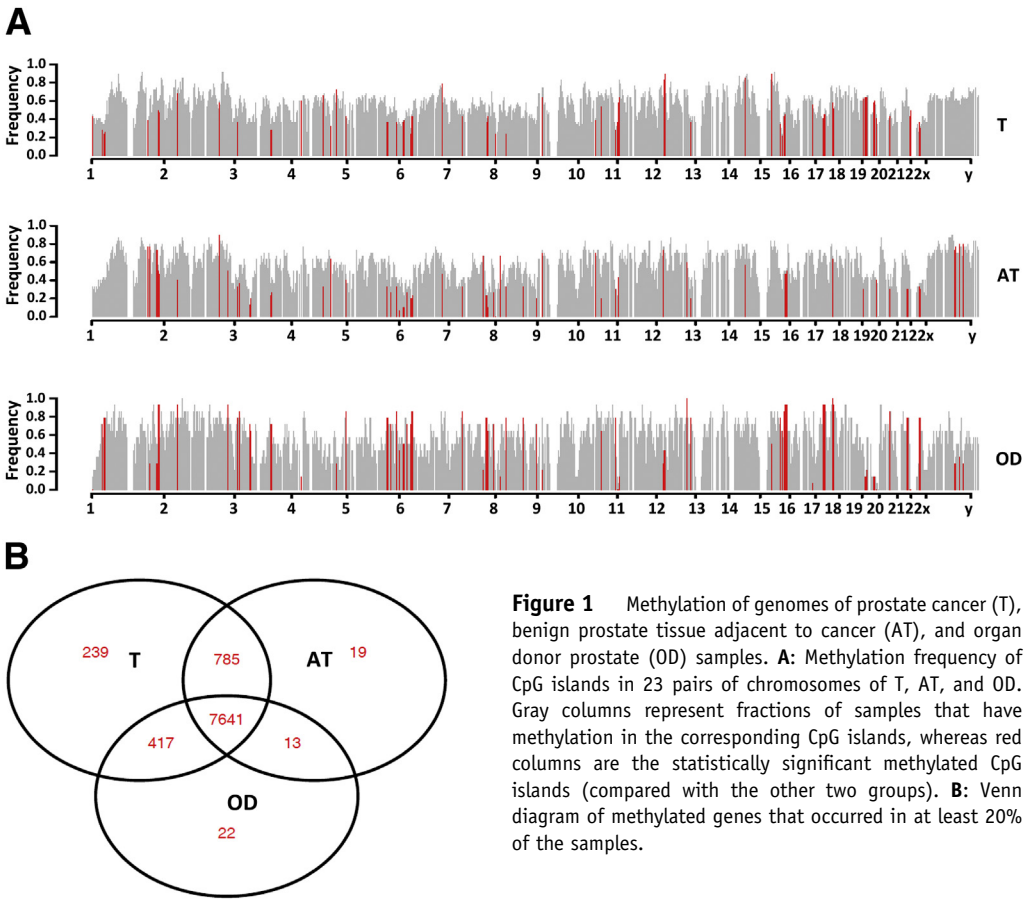

Figure 1 Methylation of genomes of prostate cancer (T), benign prostate tissue adjacent to cancer (AT), and organ donor prostate (OD) samples. **A:** Methylation frequency of CpG islands in 23 pairs of chromosomes of T, AT, and OD. Gray columns represent fractions of samples that have methylation in the corresponding CpG islands, whereas red columns are the statistically significant methylated CpG islands (compared with the other two groups). **B:** Venn diagram of methylated genes that occurred in at least 20% of the samples.

presence of gene-associated CpG islands. CpG islands located within 1000 bp upstream and 500 bp downstream of the mRNA start site of a gene were considered potentially functional and were included. Based on these criteria, 11,481 potentially functional CpG islands were identified along with a total of 9136 genes. Among the gene-associated CpG islands, 9082 were found to be methylated in T, 8458 in AT, and 8093 in OD samples.

To investigate the differential methylation status of prostate cancer-related CpG islands, the data were classified into groups of T ($n = 47$), AT ($n = 30$), and OD ($n = 14$) and compared in pairs for each CpG island identified. The proportion of each group's samples that showed methylation in each gene-associated CpG island assessed was determined, and the distributions of these CpG islands in different chromosomes are shown in Figure 1A. By comparing three group pairs (T/OD + AT, AT/T + OD, and OD/T + AT), the differentially methylated CpG islands ($P < 0.01$) in T were identified in comparison with OD or AT (Figure 1A). Similarly, the genes associated with CpG islands that were differentially methylated in AT or OD were identified (Figure 1A). The number of genes that had at least one associated CpG island and were found to be methylated in at least 20% of samples in each patient group is shown in a Venn diagram (Figure 1B). Many of these methylated segments were not unique and overlapped with at least one of the other groups. A total of 7641 genes were methylated in all three groups (T, AT, and OD). Genes (785) were methylated in the T and AT groups but not in the OD group. Only 239 genes were methylated in the T group only, compared with the 19 and 22 genes that were uniquely methylated in the AT and OD groups, respectively. The differentially methylated genes between the T and OD groups mainly clustered in regions of chromosomes 1, 3, 15, and 17 (Figure 2). Interestingly, the T and AT groups shared many of the same differentially methylated genes, which were not methylated in the OD group. Few genes were detected with differential methylation between the T group and the AT group. To rule out the effect of age on methylation pattern, samples from patients and organ donors of age 50 years were analyzed in an age-matched manner. The results also suggested a significant field effect: 110 CpG islands were found uniquely methylated in the T group, whereas only 27 were in the AT group and 25 in the OD group. Greater than 79% (423 of 533) of CpG islands differentially methylated in T group (versus OD) were also methylated in AT samples.

Gene methylation generally has a negative effect on gene expression. However, such effect can vary according to the characteristic of an associated CpG island, the level or position of the cytosine methylation, and other structural features. To investigate whether methylation of gene-associated CpG islands affected the corresponding gene expression, we performed a concordance analysis on differentially methylated genes with the use of gene expression data available from our previously published Affymetrix U95 expression data set.

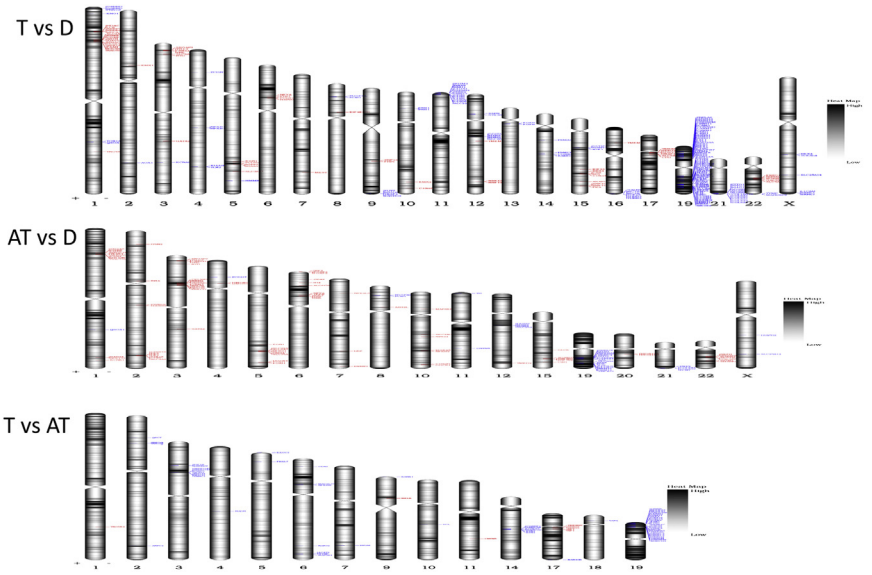

Figure 2 Ideograms of differential methylations between T, AT, and OD; T versus OD, AT versus OD, and T versus AT. **Upper panel:** Differential methylation in T (blue) and OD (red). **Middle panel:** Differential methylation in AT (blue) and OD (red). **Lower panel:** Differential methylation in T (blue) and AT (red).

These data overlapped 75 of 91 samples of the present methylation analysis. Thus, the concordance analysis largely reflected a direct methylation effect on expression. Differentially methylated genes with down-regulation of gene expression ($P < 0.01$) were designated as functional methylation. Genes with methylation but having no suppression of gene expression were considered as nonfunctional methylation. Our analyses showed that 12.5% of the differentially methylated genes are functional (Figure 3, A–C). The highest frequency of functional differential methylation occurred in the T group ($n = 47$), with the lowest occurring in the OD group ($n = 14$) (Figure 3A). In particular, 95 of 650 genes were functionally methylated in the T group, whereas only 7 of 35 were functionally methylated in the AT group. When the AT group was compared with the OD group, 23 of 315 genes were classified as differentially methylated with suppressed gene expression being detected in either the AT or OD group. Only five functional hypermethylation and one functional hypomethylation events were found when the AT group was compared with the T group. These results suggest a significant similarity between the T and AT groups in their methylation patterns.

To understand the significance of these differential DNA methylation events, pathway analyses were performed on the most significantly differentially hypermethylated and hypomethylated genes of each group (as identified by the Fisher exact test of independence, $P < 0.01$). The most frequently identified pathways corresponding to the DNA methylation and associated genes are shown in Supplemental Tables S2 and S3. Many of the hypermethylated genes in T (T/OD) were involved in inhibition of cell proliferation or cell division, such as cyclin-dependent kinase inhibitor 1C (*CDKN1C*) and *CDKN2D*, whereas the hypomethylated genes in T were involved in membrane transport. No significant pathway enrichment was identified when T was compared with AT. In AT versus OD, an apoptosis pathway was suppressed in the AT group [according to hypermethylation of some critical apoptotic genes, such as BCL2-associated X protein (*BAX*) and proteasome (prosome, macropain) 26S unit, ATPase, 4 (*PSMC4*)], whereas the membrane transport molecules were up-regulated by hypomethylation (Supplemental Table S3), although with relatively weaker statistical significance.

To investigate whether the differentially methylated genes in prostate samples are predictive of prostate cancer, we performed classification analyses with aggregated methylation data for the differentially methylated CpG islands and the prostate samples stratified as T, AT, or OD. We first ranked the differential methylation genes by *P* value. We then built and optimized our classification model by incremental inclusion of top-ranked genes into the model, until the model showed no improvement in prediction. With the use of 300 hypermethylated and 300 hypomethylated CpG islands identified in the T group, our leave-one-out classification of T versus OD showed a prediction specificity of 89.4% and a sensitivity of 85.7% (Figure 4A). Interestingly, when this prediction model was used to classify 30 of the AT samples, 80.0% (24 of 30) of the AT samples were predicted as cancer. Only six AT samples (20%) were predicted as normal, resembling a significant field effect as reported for other studies.[3] In the classification of AT versus OD, a model of 200 hypermethylated and 200 hypomethylated CpG islands was constructed, and the prediction sensitivity of AT reached 71.4% and specificity reached 100% (Figure 4B). As expected, the T versus AT classification yielded no statistically significant correct predictions.

Next, the LOOCVs were applied to predict the clinical outcomes of prostate cancer samples. The cases of prostate cancer were subdivided into groups of patients who relapsed after radical prostatectomy and patients who had no relapse for at least 5 years after the surgery. With the use of 20 differentially hypermethylated and 20 hypomethylated CpG islands for the prostate cancer relapse samples, the prediction specificity was 85.2% and sensitivity was 80.0% (Figure 5A) for prostate cancer relapse. When the prostate cancer samples were subdivided into fast relapsing [prostate-specific antigen

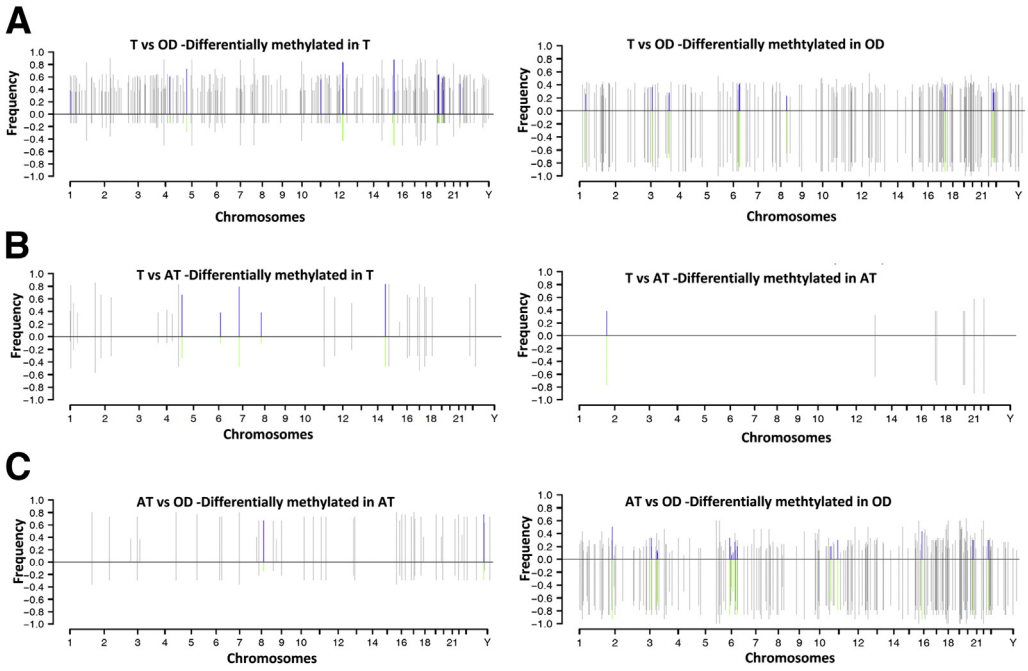

Figure 3 Functional and differential methylation between T, AT, and OD. **A**: Differential methylation of CpG islands between T and OD. **Left panel**: CpG islands differentially methylated in T samples (positive) versus OD (negative). Blue indicates CpG methylation associated with down-regulation of gene expression in T samples. **Right panel**: CpG islands differentially methylated in OD samples (negative) versus T (positive). Green indicates CpG methylation associated with down-regulation of gene expression in OD samples. **B**: Differential methylation of CpG islands between T and AT. **Left panel**: CpG islands differentially methylated in T samples (positive) versus AT (negative). Blue indicates CpG methylation associated with down-regulation of gene expression in T samples. **Right panel**: CpG islands differentially methylated in AT samples (negative) versus T (positive). Green indicates CpG methylation associated with down-regulation of gene expression in AT samples. **C**: Differential methylation of CpG islands between AT and OD. **Left panel**: CpG islands differentially methylated in AT samples (positive) versus OD (negative). Blue indicates CpG methylation associated with down-regulation of gene expression in AT samples. **Right panel**: CpG islands differentially methylated in OD samples (negative) versus AT (positive). Green indicates CpG methylation associated with down-regulation of gene expression in OD samples.

doubling time (PSADT) of 4 months] and nonfast relapse groups (nonrelapse or relapse with PSADT $\geq$15 months), the prediction specificity was 88.9% and sensitivity was 78.9% for fast relapse, using as few as 20 hypermethylated and 20 hypomethylated CpG islands identified from fast relapse tumors (Figure 5B).

To validate the findings of methylated DNA, the *CDKN1C* gene was selected for methylation-specific PCR analysis. As indicated in Figure 6, A and B, the amplified methylated CDKN1c products were detected in most of the tumor samples, and both methylated and unmethylated amplicons were detected in the PC3 cell line and a number of tumor samples.

Discussion

Systematic analyses of gene methylation of prostate cancer have been performed with various approaches, including hybridization of sodium bisulfite-treated DNA to predesigned oligo probe set[32] or extension by predesigned primers,[33] or deep sequencing of methylated CpG-enriched DNA.[34] These high throughput analyses were performed with various commercial or institutional specific platforms and revealed various methylation patterns in prostate cancer.[32,34,35] Anti-methylcytosine antibody enrichment of methylated DNA had been used to perform whole genome methylation analyses. It had been successfully validated in several studies.[36–39] With the use of a similar strategy, our genome methylation analysis revealed distinct patterns of genome methylation in several types of prostate tissues. No significant preference was observed toward high or low density of methylated CpG

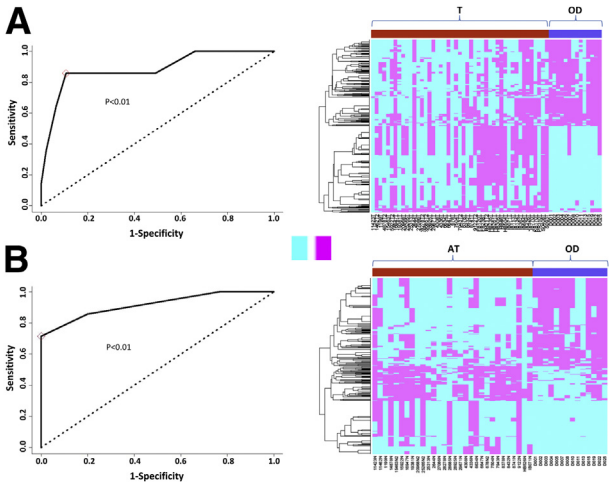

Figure 4 Classification of prostate samples based on differential methylation. **A**: Classification of T versus OD samples on the basis of 300 differentially methylated genes; ROC curve (**left**); methylation heat map (pink indicates methylation and blue nonmethylation) (**right**). **B**: Classification of AT versus OD samples on the basis of 800 differentially methylated genes; ROC curve (**left**); methylation heat map (pink indicates methylation and blue nonmethylation) (**right**).

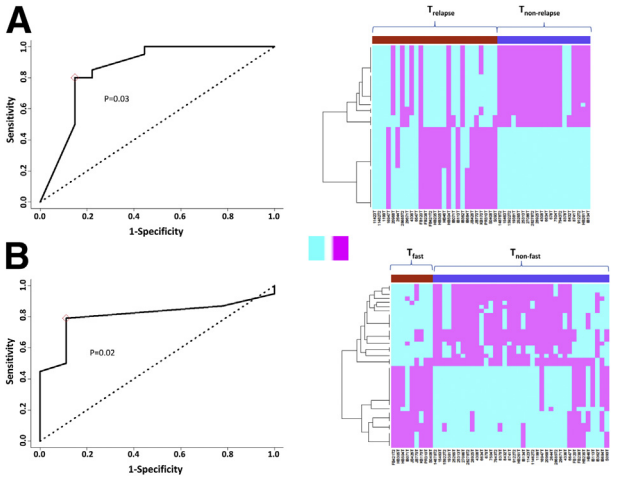

Figure 5 Prediction of clinical outcomes of prostate samples on the basis of differential methylation. **A:** Prediction of relapse versus no relapse for at least 5 years from prostate cancer samples on the basis of 40 differentially methylated genes; ROC curve (**left**); methylation heat map (pink indicates methylation and blue nonmethylation) (**right**). **B:** Prediction of fast relapse (PSADT <4 months) versus nonfast relapse from prostate cancer samples on the basis of 40 differentially methylated genes; ROC curve (**left**); methylation heat map (pink indicates methylation and blue nonmethylation) (**right**).

islands on the basis of similar average CpG counts ($n = 15$) per 100 bp in a methylated CpG island detected in our assays versus that (15.1) of all CpG islands in the human genome.

Epigenetic modification of DNA, such as cytosine methylation in CpG dinucleotides, is one of the most important regulatory mechanisms of gene expression. Promoter DNA methylation, in particular, is critical for controlling genes involved in cell cycle progression, cell survival, DNA damage repair, and other signal transductions, and these genes are often found to be silenced in clinical cancer samples.[15–23] However, information about gene methylation in prostate cancer is still fragmented. No global functional analyses have been performed to analyze whether gene methylations have an effect on gene expressions. To our knowledge, this is the first report that systematically analyzes the effects of CpG island methylations on gene expressions. Our study suggests that the number of nonfunctional CpG islands is much larger than previously thought.[32,40]

For many genes studied to date, methylation-induced gene silencing has been attributed to the methylation of CpG clusters in the promoter and exon 1 regions. Previous studies of clinical samples of prostate cancer have shown that large numbers of genes are down-regulated.[4,41–43] However, our methylation/expression concordance analyses showed that only a small fraction (12.5%) of the methylated CpG islands is functional, as evidenced by methylations accompanied by down-regulated expression of the same genes. This analysis suggests that not all CpG island methylations affect gene expression. Additional factors, such as methylation density or specific dinucleotide methylation, or the characteristics of the CpG islands themselves may account for the different effects on transcriptional activity. These functional CpG islands may have significant clinical implications. Unlike genome structural alterations, such as deletion or mutation, DNA methylations are potentially reversible. Several epigenetic treatments are currently available to reverse these modifications and have been assessed for their potential to treat cancers.[43–46]

Interestingly, the differentially methylated genes with down-regulated expression in the T samples are enriched in signaling pathways of cell cycle progression, mitogenic processes, apoptosis, and membrane transporters. Concordant methylation/low expression events in two cyclin D-dependent kinase inhibitors, *CDKN1C* and *CDKN2D*,[47–49] occurred with frequencies of 48.0% and 44.0%, respectively. These two genes are known to block cell cycle entry from G_1 to S phase, thereby inhibiting cell growth and proliferation. In addition, the cell growth inhibitor with ring finger domain 1 (CGRRF1),[50] which acts as a p53 responsive protein in cell growth arrest, was also methylated and down-regulated, suggesting a synergistic action of these genes regulated by methylation in tumors. Methylation-mediated silencing of the DNA-damage-inducible transcript 3 (DDIT3)[51,52] has been reported to suppress the ability of cells to adequately respond to stresses. These perturbed functions may lead to genome instability in the tumor. In addition, it is intriguing to find that the differentially methylated genes include a family of tumor suppressor genes, tissue inhibitor of metalloproteinase 3 (TIMP1) to TIMP3. TIMP3 is a protein suppressing metalloproteinase that degrades extracellular matrix.[53,54] TIMP1 gene promoter was previously found methylated in prostate cancer, and the loss of TIMP1 protein while gaining metalloproteinase has been attributed to the high motility of tumor cells.[54,55] Frequent methylation of TIMP1 (53%), TIMP2 (21%), and TIMP3 (6%) genes in prostate cancer in our study suggests a concerted effect of inactivation of inhibitors of metalloproteinase. This may enable cancer cells to migrate and to invade into adjacent tissues. However, the

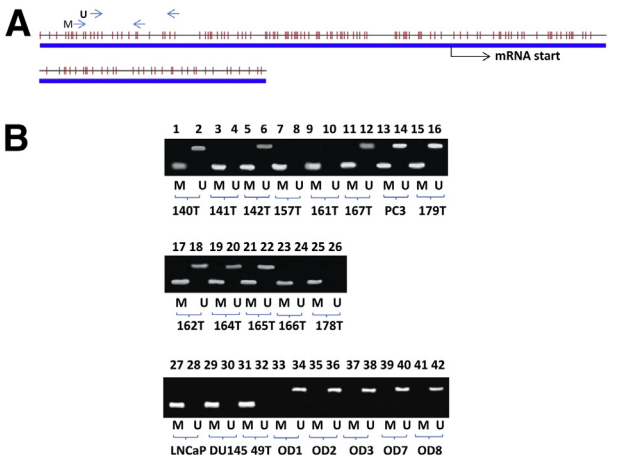

Figure 6 Methylation-specific PCR of CDKN1c CpG islands. **A:** Schematic diagram of CpG islands in the promoter and exon 1 regions of CDKN1c. CpG dinucleotides are indicated by the small red bar. The thick blue line represents the span of the CpG island. U denotes primers designed for unmethylated sequence, and M indicates methylated sequence. The mRNA start site is indicated by an **arrow. B:** Methylation-specific PCR of prostate samples. The suffix T denotes prostate cancers, and the suffix OD denotes organ donor prostates.

discovery of methylation of some of the mitogenic genes, such as fibroblast growth factor 9 (FGF9)[56,57] and mitogen-activated protein kinase 8 interacting protein 2 (MAPK8IP2), in prostate cancer samples indicates a complicated pattern of cancer methylation.

Previous studies suggest significant field effect of prostate cancer through systematic genome methylation analyses.[32–34] The methylation patterns in T and AT in our analyses were remarkably similar, although there were uniquely methylated genes identified in T. Few genes were found to be differentially methylated in the prostate cancer versus benign tissues adjacent to prostate cancer. The differences between organ donor prostate samples and benign prostate tissues adjacent to cancer, however, were highly significant, suggesting that alterations of gene methylation precede the morphologic malignancy. These findings suggest a strong field effect in prostate cancer, similar to that found in the gene expression and genome analyses.[3] The similarities between these two groups (T and AT) suggest that epigenetic alterations occurred much earlier than previously thought.

Finally, our classification and prediction analyses with the use of the differentially methylated genes in prostate cancer yields an excellent prediction rate for tumor samples with relapse (compared with nonrelapse samples) or for tumor samples that have a short PSADT (compared with samples having longer times). To our knowledge, this is the first report to suggest that a differential methylation profile can be used for prostate tumor prediction or prognostic evaluation with high fidelity. Because methylation modification is a reversible process, the prostate cancer-related hypermethylation and hypomethylation genes identified in this study may represent candidate targets for clinical therapeutic intervention.

Acknowledgment

We thank Chia-Yueh Yen for her technical support.

J.-H.L., G.M., J.N., and Y.P.Y. conceived the idea. J.-H.L. and Y.P.Y. directed and performed the experiments. Y.P.Y., J.-H.L., and G.T. developed the strategy to analyze the data. Y.D. and R.C. performed the statistical analyses.

Supplemental Data

Supplemental material for this article can be found at *http://dx.doi.org/10.1016/j.ajpath.2013.02.040*.

References

1. Siegel R, Naishadham D, Jemal A: Cancer statistics, 2012. CA Cancer J Clin 2012, 62:10–29
2. Yu YP, Landsittel D, Jing L, Nelson J, Ren B, Liu L, McDonald C, Thomas R, Dhir R, Finkelstein S, Michalopoulos G, Becich M, Luo JH: Gene expression alterations in prostate cancer predicting tumor aggression and preceding development of malignancy. J Clin Oncol 2004, 22:2790–2799
3. Yu YP, Song C, Tseng G, Ren BG, Laframboise W, Michalopoulos G, Nelson J, Luo JH: Genome abnormalities precede prostate cancer and predict clinical relapse. Am J Pathol 2012, 180:2240–2248
4. Luo JH, Yu YP, Cieply K, Lin F, Deflavia P, Dhir R, Finkelstein S, Michalopoulos G, Becich M: Gene expression analysis of prostate cancers. Mol Carcinog 2002, 33:25–35
5. Magee JA, Araki T, Patil S, Ehrig T, True L, Humphrey PA, Catalona WJ, Watson MA, Milbrandt J: Expression profiling reveals hepsin overexpression in prostate cancer. Cancer Res 2001, 61:5692–5696
6. Luo JH: Gene expression alterations in human prostate cancer. Drugs Today (Barc) 2002, 38:713–719
7. Ernst T, Hergenhahn M, Kenzelmann M, Cohen CD, Ikinger U, Kretzler M, Hollstein M, Grone HJ: [Gene expression profiling in prostatic cancer]. German. Verh Dtsch Ges Pathol 2002, 86:165–175
8. Glinsky GV, Glinskii AB, Stephenson AJ, Hoffman RM, Gerald WL: Gene expression profiling predicts clinical outcome of prostate cancer. J Clin Invest 2004, 113:913–923
9. Monk M, Grant M: Preferential X-chromosome inactivation, DNA methylation and imprinting. Dev Suppl 1990, 55–62
10. Hu JF, Vu TH, Hoffman AR: Promoter-specific modulation of insulin-like growth factor II genomic imprinting by inhibitors of DNA methylation. J Biol Chem 1996, 271:18253–18262
11. Yu G, Tseng GC, Yu YP, Gavel T, Nelson J, Wells A, Michalopoulos G, Kokkinakis D, Luo JH: CSR1 suppresses tumor growth and metastasis of prostate cancer. Am J Pathol 2006, 168:597–607
12. Yu YP, Yu G, Tseng G, Cieply K, Nelson J, Defrances M, Zarnegar R, Michalopoulos G, Luo JH: Glutathione peroxidase 3, deleted or methylated in prostate cancer, suppresses prostate cancer growth and metastasis. Cancer Res 2007, 67:8043–8050
13. Lund AH, van Lohuizen M: Epigenetics and cancer. Genes Dev 2004, 18:2315–2335
14. Bird A: DNA methylation patterns and epigenetic memory. Genes Dev 2002, 16:6–21
15. Graff JR, Herman JG, Lapidus RG, Chopra H, Xu R, Jarrard DF, Isaacs WB, Pitha PM, Davidson NE, Baylin SB: E-cadherin expression is silenced by DNA hypermethylation in human breast and prostate carcinomas. Cancer Res 1995, 55:5195–5199
16. Herman JG, Merlo A, Mao L, Lapidus RG, Issa JP, Davidson NE, Sidransky D, Baylin SB: Inactivation of the CDKN2/p16/MTS1 gene is frequently associated with aberrant DNA methylation in all common human cancers. Cancer Res 1995, 55:4525–4530
17. Kito H, Suzuki H, Ichikawa T, Sekita N, Kamiya N, Akakura K, Igarashi T, Nakayama T, Watanabe M, Harigaya K, Ito H: Hypermethylation of the CD44 gene is associated with progression and metastasis of human prostate cancer. Prostate 2001, 49:110–115
18. Vanaja DK, Cheville JC, Iturria SJ, Young CY: Transcriptional silencing of zinc finger protein 185 identified by expression profiling is associated with prostate cancer progression. Cancer Res 2003, 63:3877–3882
19. Woodson K, Hayes R, Wideroff L, Villaruz L, Tangrea J: Hypermethylation of GSTP1, CD44, and E-cadherin genes in prostate cancer among US Blacks and Whites. Prostate 2003, 55:199–205
20. Yoshiura K, Kanai Y, Ochiai A, Shimoyama Y, Sugimura T, Hirohashi S: Silencing of the E-cadherin invasion-suppressor gene by CpG methylation in human carcinomas. Proc Natl Acad Sci U S A 1995, 92:7416–7419
21. Bastian PJ, Yegnasubramanian S, Palapattu GS, Rogers CG, Lin X, De Marzo AM, Nelson WG: Molecular biomarker in prostate cancer: the role of CpG island hypermethylation. Eur Urol 2004, 46:698–708
22. Nakayama M, Gonzalgo ML, Yegnasubramanian S, Lin X, De Marzo AM, Nelson WG: GSTP1 CpG island hypermethylation as a molecular biomarker for prostate cancer. J Cell Biochem 2004, 91:540–552
23. Kang GH, Lee S, Lee HJ, Hwang KS: Aberrant CpG island hypermethylation of multiple genes in prostate cancer and prostatic intraepithelial neoplasia. J Pathol 2004, 202:233–240
24. Nalesnik MA, Tseng G, Ding Y, Xiang GS, Zheng ZL, Yu Y, Marsh JW, Michalopoulos GK, Luo JH: Gene deletions and

amplifications in human hepatocellular carcinomas: correlation with hepatocyte growth regulation. Am J Pathol 2012, 180:1495−1508
25. Jones PA, Takai D: The role of DNA methylation in mammalian epigenetics. Science 2001, 293:1068−1070
26. Takai D, Jones PA: The CpG island searcher: a new WWW resource. In Silico Biol 2003, 3:235−240
27. Takai D, Jones PA: Comprehensive analysis of CpG islands in human chromosomes 21 and 22. Proc Natl Acad Sci U S A 2002, 99:3740−3745
28. Subramanian A, Tamayo P, Mootha VK, Mukherjee S, Ebert BL, Gillette MA, Paulovich A, Pomeroy SL, Golub TR, Lander ES, Mesirov JP: Gene set enrichment analysis: a knowledge-based approach for interpreting genome-wide expression profiles. Proc Natl Acad Sci U S A 2005, 102:15545−15550
29. Golub TR, Slonim DK, Tamayo P, Huard C, Gaasenbeek M, Mesirov JP, Coller H, Loh ML, Downing JR, Caligiuri MA, Bloomfield CD, Lander ES: Molecular classification of cancer: class discovery and class prediction by gene expression monitoring. Science 1999, 286:531−537
30. Kobatake T, Yano M, Toyooka S, Tsukuda K, Dote H, Kikuchi T, Toyota M, Ouchida M, Aoe M, Date H, Pass HI, Doihara H, Shimizu N: Aberrant methylation of p57KIP2 gene in lung and breast cancers and malignant mesotheliomas. Oncol Rep 2004, 12:1087−1092
31. Shin JY, Kim HS, Park J, Park JB, Lee JY: Mechanism for inactivation of the KIP family cyclin-dependent kinase inhibitor genes in gastric cancer cells. Cancer Res 2000, 60:262−265
32. Yu YP, Paranjpe S, Nelson J, Finkelstein S, Ren B, Kokkinakis D, Michalopoulos G, Luo JH: High throughput screening of methylation status of genes in prostate cancer using an oligonucleotide methylation array. Carcinogenesis 2005, 26:471−479
33. Kobayashi Y, Absher DM, Gulzar ZG, Young SR, McKenney JK, Peehl DM, Brooks JD, Myers RM, Sherlock G: DNA methylation profiling reveals novel biomarkers and important roles for DNA methyltransferases in prostate cancer. Genome Res 2011, 21:1017−1027
34. Kim JH, Dhanasekaran SM, Prensner JR, Cao X, Robinson D, Kalyana-Sundaram S, Huang C, Shankar S, Jing X, Iyer M, Hu M, Sam L, Grasso C, Maher CA, Palanisamy N, Mehra R, Kominsky HD, Siddiqui J, Yu J, Qin ZS, Chinnaiyan AM: Deep sequencing reveals distinct patterns of DNA methylation in prostate cancer. Genome Res 2011, 21:1028−1041
35. Kron K, Pethe V, Briollais L, Sadikovic B, Ozcelik H, Sunderji A, Venkateswaran V, Pinthus J, Fleshner N, van der Kwast T, Bapat B: Discovery of novel hypermethylated genes in prostate cancer using genomic CpG island microarrays. PloS One 2009, 4:e4830
36. Kelkar A, Deobagkar D: A novel method to assess the full genome methylation profile using monoclonal antibody combined with the high throughput based microarray approach. Epigenetics 2009, 4:415−420
37. Cerf A, Cipriany BR, Benitez JJ, Craighead HG: Single DNA molecule patterning for high-throughput epigenetic mapping. Anal Chem 2011, 83:8073−8077
38. Lisanti S, von Zglinicki T, Mathers JC: Standardization and quality controls for the methylated DNA immunoprecipitation technique. Epigenetics 2012, 7:615−625
39. Komashko VM, Acevedo LG, Squazzo SL, Iyengar SS, Rabinovich A, O'Geen H, Green R, Farnham PJ: Using ChIP-chip technology to reveal common principles of transcriptional repression in normal and cancer cells. Genome Res 2008, 18:521−532
40. Goering W, Kloth M, Schulz WA: DNA methylation changes in prostate cancer. Methods Mol Biol 2012, 863:47−66
41. Tseng GC, Cheng C, Yu YP, Nelson J, Michalopoulos G, Luo JH: Investigating multi-cancer biomarkers and their cross-predictability in the expression profiles of multiple cancer types. Biomark Insights 2009, 4:57−79
42. LaTulippe E, Satagopan J, Smith A, Scher H, Scardino P, Reuter V, Gerald WL: Comprehensive gene expression analysis of prostate cancer reveals distinct transcriptional programs associated with metastatic disease. Cancer Res 2002, 62:4499−4506
43. Dhanasekaran SM, Barrette TR, Ghosh D, Shah R, Varambally S, Kurachi K, Pienta KJ, Rubin MA, Chinnaiyan AM: Delineation of prognostic biomarkers in prostate cancer. Nature 2001, 412: 822−826
44. Duan H, Zhang HJ, Yang JQ, Oberley LW, Futscher BW, Domann FE: MnSOD up-regulates maspin tumor suppressor gene expression in human breast and prostate cancer cells. Antioxid Redox Signal 2003, 5:677−688
45. Nakayama T, Watanabe M, Yamanaka M, Hirokawa Y, Suzuki H, Ito H, Yatani R, Shiraishi T: The role of epigenetic modifications in retinoic acid receptor beta2 gene expression in human prostate cancers. Lab Invest 2001, 81:1049−1057
46. Xiang N, Zhao R, Song G, Zhong W: Selenite reactivates silenced genes by modifying DNA methylation and histones in prostate cancer cells. Carcinogenesis 2008, 29:2175−2181
47. Riccio A, Cubellis MV: Gain of function in CDKN1C. Nat Genet 2012, 44:737−738
48. Giovannini C, Gramantieri L, Minguzzi M, Fornari F, Chieco P, Grazi GL, Bolondi L: CDKN1C/P57 is regulated by the Notch target gene Hes1 and induces senescence in human hepatocellular carcinoma. Am J Pathol 2012, 181:413−422
49. Okuda T, Hirai H, Valentine VA, Shurtleff SA, Kidd VJ, Lahti JM, Sherr CJ, Downing JR: Molecular cloning, expression pattern, and chromosomal localization of human CDKN2D/INK4d, an inhibitor of cyclin D-dependent kinases. Genomics 1995, 29:623−630
50. Madden SL, Galella EA, Riley D, Bertelsen AH, Beaudry GA: Induction of cell growth regulatory genes by p53. Cancer Res 1996, 56:5384−5390
51. Pereira RC, Delany AM, Canalis E: CCAAT/enhancer binding protein homologous protein (DDIT3) induces osteoblastic cell differentiation. Endocrinology 2004, 145:1952−1960
52. Jauhiainen A, Thomsen C, Strombom L, Grundevik P, Andersson C, Danielsson A, Andersson MK, Nerman O, Rorkvist L, Stahlberg A, Aman P: Distinct cytoplasmic and nuclear functions of the stress induced protein DDIT3/CHOP/GADD153. PloS One 2012, 7:e33208
53. Matthews FJ, Cook SD, Majid MA, Dick AD, Smith VA: Changes in the balance of the tissue inhibitor of matrix metalloproteinases (TIMPs)-1 and -3 may promote keratocyte apoptosis in keratoconus. Exp Eye Res 2007, 84:1125−1134
54. Osman M, Tortorella M, Londei M, Quaratino S: Expression of matrix metalloproteinases and tissue inhibitors of metalloproteinases define the migratory characteristics of human monocyte-derived dendritic cells. Immunology 2002, 105:73−82
55. Kenney MC, Chwa M, Atilano SR, Tran A, Carballo M, Saghizadeh M, Vasiliou V, Adachi W, Brown DJ: Increased levels of catalase and cathepsin V/L2 but decreased TIMP-1 in keratoconus corneas: evidence that oxidative stress plays a role in this disorder. Invest Ophthalmol Vis Sci 2005, 46:823−832
56. White AC, Xu J, Yin Y, Smith C, Schmid G, Ornitz DM: FGF9 and SHH signaling coordinate lung growth and development through regulation of distinct mesenchymal domains. Development 2006, 133:1507−1517
57. Iwata J, Tung L, Urata M, Hacia JG, Pelikan R, Suzuki A, Ramenzoni L, Chaudhry O, Parada C, Sanchez-Lara PA, Chai Y: Fibroblast growth factor 9 (FGF9)-pituitary homeobox 2 (PITX2) pathway mediates transforming growth factor beta (TGFbeta) signaling to regulate cell proliferation in palatal mesenchyme during mouse palatogenesis. J Biol Chem 2012, 287:2353−2363